Understanding formation mechanism of ZnO diatomic chain and multi-shell structure using physical mechanics: Molecular dynamics and first-principle simulations[†]

WANG BinBin, WANG FengChao & ZHAO YaPu[*]

State Key Laboratory of Nonlinear Mechanics (LNM), Institute of Mechanics, Chinese Academy of Sciences, Beijing 100190, China

In this paper, the possibility of the monatomic chain (MC) formation for ZnO material was studied by molecular dynamics (MD) simulation. The process of MC formation and the effects of temperature, strain rate and size were studied extensively. The tensile process can be divided to be five stages and the ZnO diatomic chain (DC) can be found. The MD results show that most atoms in MC came from the original surface of ZnO nanowires (NWs). Temperature and strain rate are two important factors affecting the process, and both high temperature and low strain rate in a certain range would be beneficial to the formation of DC. Moreover, the effects of strain rate and temperature could attribute to the Arrhenius model and the energy release mechanism. Furthermore, multi-shell structure was found for the samples under tensile strain and the layer-layer distance was about 3 Å. Our studies based on density functional theory showed that the most stable structure of ZnO DC was confirmed to be linear, and the I-V curve was also got using ATK.

Yuan and Zhao [1] explored the possibility for the formation of a stable and long gold monatomic chain (MC) by using the unique transport properties of the precursor chain in an interior corner. The investigation of the new formation methods of MC was done [1] because a single-atom chain of Au has the highest yield strength among all Au micro- and nano-structures [2,3] as shown in Figure 1, which illustrates a systematic trend of the increase in experimental yield strength of a Au nanostructure as the size is reduced towards the atomistic scale.

The first direct observation of gold MC was found in 1998 and the conductance was also studied [4]. MC has many unique properties such as the smallest electrical wire and ultimate surface-to-volume ratio. Thus MC has potential applications in electronic devices and high-performance gas-sensing devices. Moreover, MC is an ideal prototype of a nanowire (NW) for extensibility and mechanical strength study as no processes of bond unfolding or atom glide dislocating are involved in the deformation [5].

The atomic chain may possibly transport current with high density and be applied to molecular devices. Therefore, various materials such as Pt and Ni were studied experimentally and theoretically. From both experiments and calculation, NWs show quantized conductance units of $2e^2=h$, and single chains of gold atoms were confirmed to have one unit of conductance [6,7]. Many techniques such as pulling atoms with a scanning tunneling microscope (STM), separating two metals with a mechanically controllable breaking

---
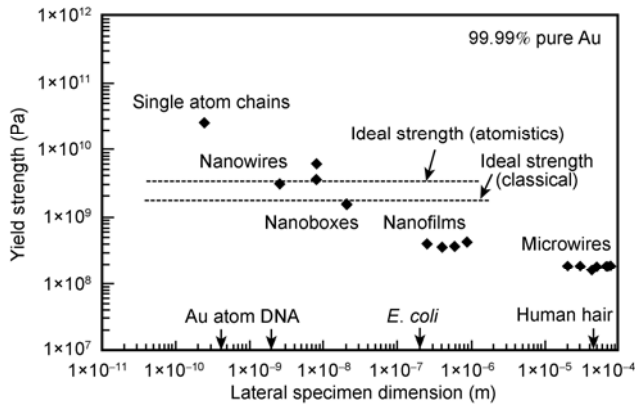
Figure 1 Experimental measurement of the yield strength of Au nanostructures as a function of lateral specimen dimension [2,3].

junction, or by producing holes in a gold thin foil with a high resolution transmission electron microscope were used to produce stable chains of atoms [7–11]. The stability and longevity of gold MC was also studied which confirmed that the MC is stable in certain environment [9,12]. These experiments have motivated the theoretical studies attempting to understand the formation and evolution on monoatomic NWs. Calculation based on molecular dynamics and ab initio method have been carried out [3,8,13–15]. The magnetic properties of gold nanotubes encapsulated transition metal (TM, TM=Co and Mn) and MC have been studied using density functional theory (DFT) calculations [16]. Furthermore, many theoretical studies attempt to reveal the MC forming mechanism [17–21].

The MC has been found in many materials; however, most materials are noble metal [4,19,22]. In this paper, we present our calculation results about the formation of the diatomic chain (DC) for ZnO NW, which is a semiconducting material and attracted many focus of research. Based on classic molecular dynamics (MD) simulation, we found that the ZnO DC forms when the ZnO NW was under elongation and certain environmental conditions. Temperature and strain rate are two important factors governing the formation process of ZnO DC. Too low or too high temperature and strain rate are not beneficial to the formation of atomic chain. Comparison between samples with different dimensions shows that there exists size effect in the formation. Based on the simulation results, we found that DC is not liable to occur in small samples. However, high temperatures in a certain scope could enhance the activity of atoms thus could be beneficial to the formation of DC. Multi-shell structures were found in ZnO NWs under tensile strain. Furthermore, stable configuration and conductivity of ZnO DC are investigated in this paper. These architectures are intriguing objects for further exploration of the physical properties and possible applications of advanced molecular or atomic devices.

1 Simulation methods

We investigated the structure and mechanical properties of wurtzite ZnO NWs using MD simulations with the Buckingham type potential for atomic interactions, which has been successfully used in simulation of fracture and dislocation nucleation in ZnO nanostructures. The potential function was as follows and corresponding parameters were shown in Table 1 [23]. The first term in eq. (1) denotes the Columbic interactions due to electric charges, and the second term and the third term are both short-range interactions, which are attraction and repulsion, respectively

$$U\left(r_{ij}\right) = \frac{q_i q_j}{r_{ij}} + A\exp\left(\frac{-r_{ij}}{\rho}\right) - \frac{C}{r_{ij}^6}, \qquad (1)$$

where A, ρ and C are potential parameters, r_{ij} is the distance between two ions, and q_i is the charge on ion i. It should be noted that Einstein summation convention is not applied here, and repeated indices does not indicate summation in eq. (1).

The NW models with different cross sectional shapes were cut from the wurtzite crystal ZnO. Here, the ZnO NWs with square cross sections were considered as shown in Figure 2. According to the experiments, the

Table 1 Parameters for ZnO Buckingham potential function

Species		A (eV)	ρ (Å)	C (eV Å^6)
O^{2-}	O^{2-}	9547.96	0.22	32.00
Zn^{2+}	O^{2-}	529.70	0.36	0.00
Zn^{2+}	Zn^{2+}	0.00	0.00	0.00
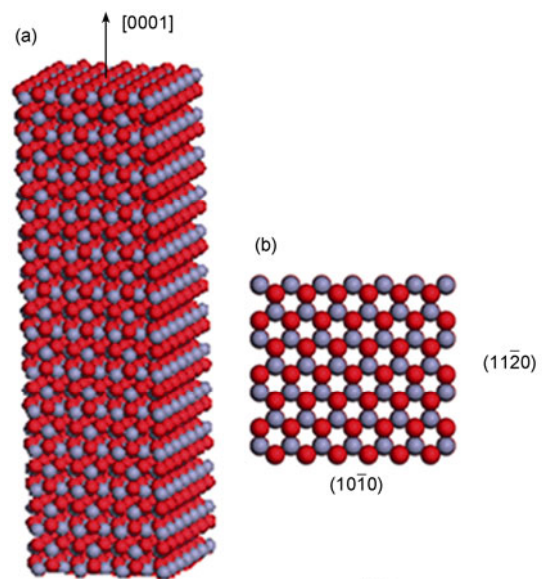
Figure 2 (Color online) Simulation model of ZnO NWs. (a) ZnO NW along [0001] direction; (b) cross-section and two facets.

axial direction of ZnO NWs is [0001] and the crystal orientations of side faces are ($10\bar{1}0$) and ($11\bar{2}0$). The NWs are relaxed to a minimum energy configuration with all free boundary conditions, and then thermally equilibrated equilibrated to 0, 300, 500, and 700 K for 30 ps using the Nosé–Hoover thermostat with a time step of 2 fs while keeping the length of the wires constant. Approximation to quasi static tensile loading in each deformation increment is achieved in two steps, including 10 ps loading process and 10 ps relaxation. The loading is applied along the axis of the NWs; with the bottom layers fixed and another tip move an increment in the length direction. Periodic boundary conditions were not used at any direction for all the simulations in this work. The velocity verlet algorithm was used to integrate the equations of motion and all MD simulations in this study were performed using the parallelized code LAMMPS [24]. The snapshots of the MD results were processed by the package of ATOMEYE [25]. Furthermore, in order to investigate the stable configuration and conductivity of ZnO DC, GAUSSION03 and ATK were employed in this article.

2   Results and discussion

2.1   Cross sections after relaxation

The ZnO NWs models were cut from the bulk wurtzite ZnO crystal, thus the atom configuration would change after relaxation. The simulation results for the ZnO NW relaxed for 30 ps under 300 K were shown in Figure 3. The sizes of cross sections are: 10 Å × 10 Å, 15 Å × 15 Å, 20 Å × 20 Å, 30 Å × 30 Å, respectively. It was found that the crystal structure cannot be maintained after relaxation for the NW with the side length less than 10 Å, and the resulting cross-section was round-like (Figures 3(a) and (b)). The crystal structure of ZnO NWs with larger size could be maintained, the results shown in Figure 3(c)–(h). Serious observation shows that only atoms which are near to the surface move inward, which may mean that the ZnO NWs make contact during relaxation. The sharp corners of square cross section become smooth, and the inner atoms maintain the original structures.

2.2   Multi-shell structure of ZnO NWs after relaxation under tensile stress

The Multi-shell structure was found on sample with cross section: 15 Å × 15 Å and 300 K and the structures formed under tensile stress, which is a key factor in transition. From the viewpoint of crystal structure, the surface atoms from planes ($10\bar{1}0$) and ($11\bar{2}0$) reconstruct forming rings that compose the rounded surface of NWs, which is a ($10\bar{1}0$)
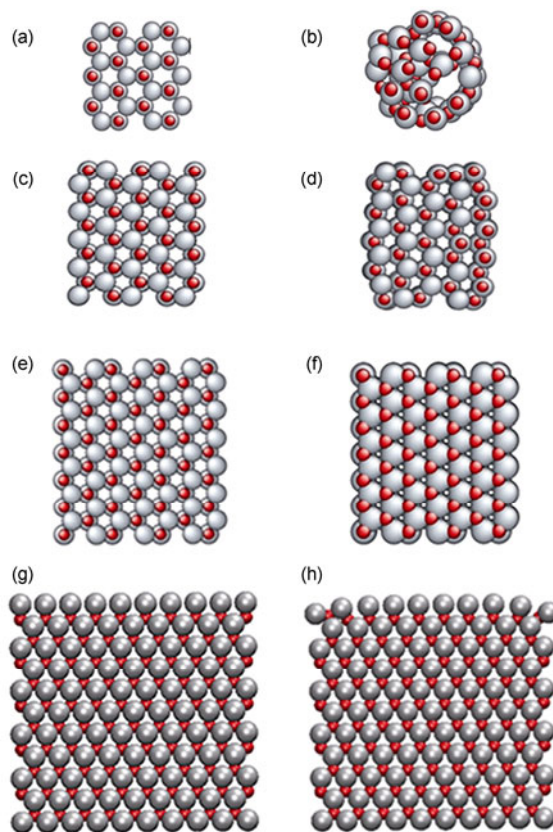
Figure 3   (Color online) Cross section shape of ZnO NWs with different size before and after relaxation. (a) 10 Å × 10 Å before relaxation; (b) 10 Å × 10 Å after relaxation; (c) 15 Å × 15 Å before relaxation; (d) 15 Å × 15 Å after relaxation; (e) 20 Å × 20 Å before relaxation; (f) 20 Å × 20 Å after relaxation; (g) 30 Å × 30 Å before relaxation; (h) 30 Å × 30 Å after relaxation.

surface displaying hexagons. Conversely, (0001) planes are very compact with shorter bonds than those from other planes. When the NW is under tension along the [0001] direction, the compact (0001) planes relax to form rings, keeping registry of their initial angular arrangement. As a consequence, the outermost shell that would otherwise expose facets reconstructs into a rounded ($10\bar{1}0$) surface, which has the lowest free energy for wurtzite ZnO [13]. The first stage of the evolution of the NW is shown in Figure 4(a), which presents the evolution of ZnO NW formed in the [0001] direction. Before relaxation it exhibits ($10\bar{1}0$) and ($11\bar{2}0$) facets, which become a rounded surface after relaxation. The atoms rearrange by slipping to accommodate the round formation to become ($10\bar{1}0$) rounded surfaces. The process of ring formation also involves rounding the inner planar facets into ring-type structures, thus the ZnO NWs show multi-shell structure and each layer becomes a round like ($10\bar{1}0$) surface. Furthermore, we observe that distance between each ring is approximately 2.9–3.4 Å (Figure 4(d)), which is much less than the bond length in bulk wurtzite ZnO crystal (1.992 and 1.973 Å).
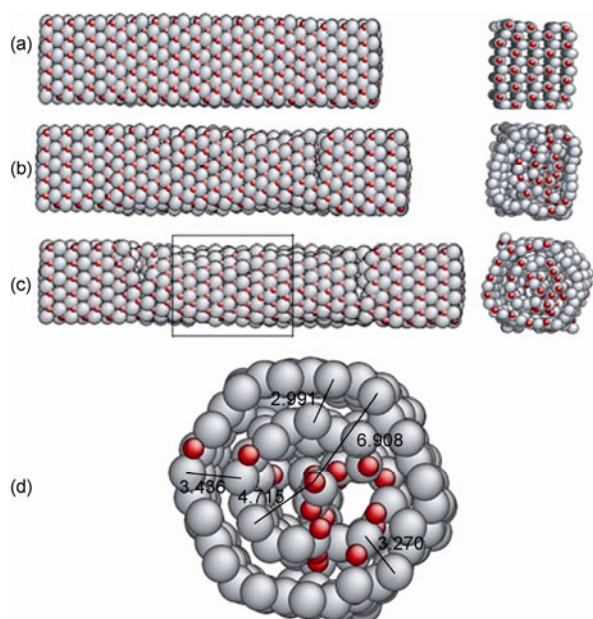
Figure 4 (Color online) Multi-shell structure of ZnO NWs under tensile strain. (a) Initial state; (b) intermediate state; (c) round like multi-shell structure; (d) distances between each shell.

This result may indicate that the attractive force between layers are relative small, thus slip between shells may exist during the tensile process.

2.3 Formation of ZnO DC

Based on the simulation results, the ZnO DC forms with the development of tensile process. One typical formation process (cross section: 20 Å × 20 Å NW, temperature: 500 K, strain rate: 2.08×10^9 s^{-1}) was shown in Figure 5(a)–(e), which could be divided into five distinct stages:

Stage 1: (nominal strain 0–6.87%): The crystal structure of NW has not been destroyed and the NW endures uniform deformation;

Stage 2: (nominal strain 6.87%–26.45%): Necking occurs, and propagated with the tensile process;

Stage 3: (nominal strain 26.45%–60.41%): ZnO DC forms, and the atom number on the DC increases with elongation；

Stage 4: (nominal strain 60.41%–64.57%): Number of atoms on DC maintains constant, and the DC is pulled tight gradually;

Stage 5: Fracture occurs and the DC contracts.

Further investigation shows two characteristics during the process. Firstly, most atoms on diatomic chain come from the original surface of ZnO NW [15]. In order to investigate the movement of atoms in ZnO NWs, we marked the inner atoms and the surface atoms with different colors, as shown in Figure 6(a). It was found that the atoms In ZnO DC are largely from the surface of ZnO NWs (Figure 6(b)). We attribute this phenomenon to the fact that the atoms on
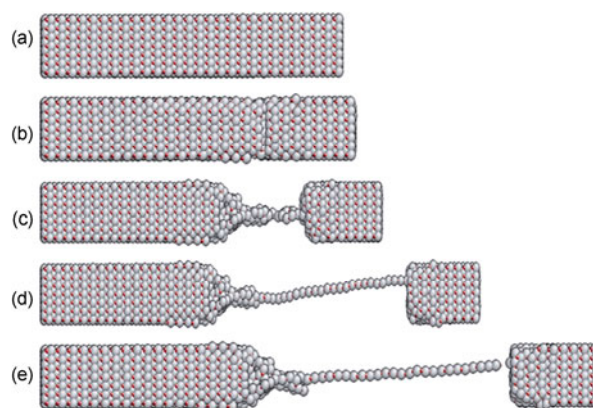
Figure 5 (Color online) Five stages during the tensile process. (a) Homogeneous deformation stage; (b) occurrence and propagation of necking; (c) occurrence of DC; (d) the atom number on DC mains and the chain was stretched gradually; (e) rupture and contract of DC.
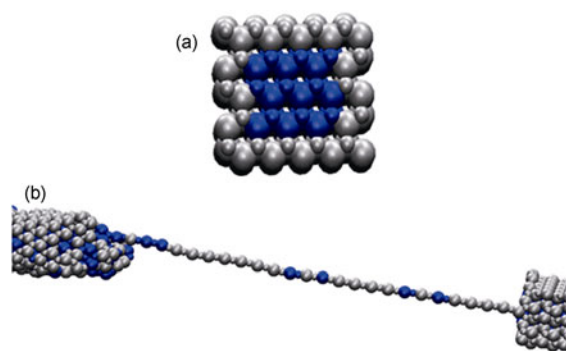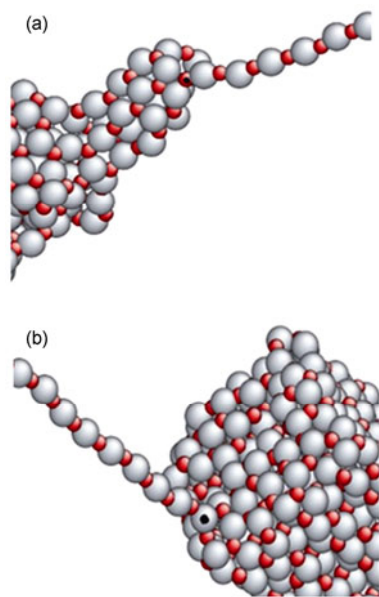

Figure 6 (Color online) Origin of the atoms on ZnO DC. (a) Cross-section of the ZnO NW before the tensile process, the inner atoms and the surface atoms were marked with different colors; (b) formation of the ZnO DC.

the surface are more liable to slip than inner ones for the adjacent atoms are fewer. Therefore, inner atoms could maintain the crystal structure while surface atoms slip into the DC during the elongation process.

Secondly, the tips of the DC were found to be pyramid-like on the one end (Figure 7(a)) and cliff-like on the opposite end (Figure 7(b)). The pyramid tip comes from the necking part, and the surface atoms slipped in to the tip gradually. The atoms were pulled in to DC from the pyramid tip. The other end shows a cliff shape, and no pyramid-like tip was found. The reason may be that the geometrical positions of holding part are fixed in the model. The basic principle for the rupture of DC is that the force to pull out new atoms from "pyramid" tip is larger than the rupture force of ZnO bond. Further investigation on the rupture force of Zn-O bond is determined to be about 3.12 nN. It is comparable with the rupture force of about 1.2 nN for a gold-gold bond obtained in Car-Parrinello molecular dynamics (CPMD) simulations for pulling monatomic gold chain from Parrinello's group [26].
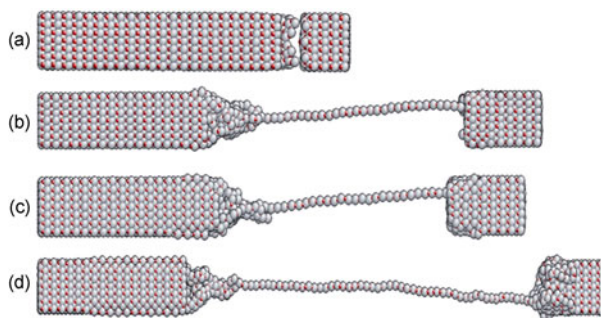
2.4 Temperature and strain rate effects
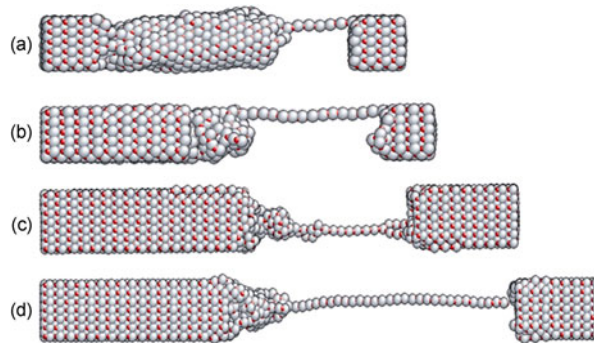
As the temperature governs the activity of atoms, very low

Figure 7   (Color online) Two ends of the ZnO DC. (a) "pyramid" tip; (b) "cliff" tip.

Figure 9   (Color online) Strain rate effects of two typical samples. (a) 15 Å × 15 Å and 2.08×10^8 s^{-1}; (b) 15 Å × 15 Å and 2.08×10^9 s^{-1}; (c) 20 Å × 20 Å and 2.08×10^8 s^{-1}; (d) 20 Å × 20 Å and 2.08×10^9 s^{-1}.

temperatures would constrain the movements of Zn and O atoms. Thus, it was well-known that ZnO DC will not come into being when ZnO NWs was stretched under very low temperature (that is 0.01 K). Sun [5] predict that the melting point of MC was proportional to the bond energy of atoms, whose coordination number is only two. Thus the melting point of MC is much lower than the bulk material. Too high temperature is not suitable for the formation of ZnO DC as the ZnO was in a possible liquid state [27]. The ZnO DCs under different temperatures are shown in Figures 8(a)–(d), in the temperatures of 0, 300, 500 and 700 K, respectively. The MD simulation results are in good agreement with theoretical predictions.

The strain rate effect was calculated under two conditions: 2.08 ×10^8 s^{-1} and 2.08 ×10^9 s^{-1}, respectively. According to the calculation results, the ZnO DC under higher strain rate would be longer than the one under lower strain rate as shown in Figure 9, which may be considered as the forma-

tion of ZnO DC, liable to occur under high strain rate. The simulation temperature is 300 K and the cross sections of two samples are 15Å × 15 Å and 20 Å × 20 Å. The calculation results are shown in Figure 9. However, we could assume that the ZnO NW would rupture without much deformation under very high strain rate. The formation process of ZnO DC has some similarity compared with the formation of natural silk. Tensile force is crucial for the formation of DC and silk. It was found that the silkworm could not produce silk while keeping its head steady. Thus, silk was pulled from the body of silkworm. Moderate strength is another important factor. Interactions between Zn atoms and O atoms ensure the strength and moderate elasticity of DC. Under high strain rates, the ZnO NWs show fluid-like behavior and ZnO DC was in neither solid state nor liquid state.

2.5   Size effect

Size effect is one important character of nanoscale objects that is different with macro mechanical problems. With the calculation results of ZnO DC formation, we can conclude DC could not form with a very small sample and a larger sample could produce a longer DC in a reasonable scope. DC is relatively short with larger samples as the inner atoms have larger restriction on the surface atoms than a smaller sample. Atoms of samples with small dimensions exhibited no-order distribution. The NW would rupture directly without much deformation and DC was short (Figure 10(a)). For the sample Figures 10(b) and (c), we can see that large samples could produce longer atomic chain as more surface atoms could be provided. Another tendency is seen in Figure 10(d). Compared with other samples, the atomic chain was much shorter. We attribute this phenomenon to the large constrain on surface atoms as the bulk atoms could maintain crystal structure largely. However, to increase the activity of surface energy by raising the temperature could be a possible solution for large samples.

Figure 8   (Color online) Temperature effects under four typical temperatures. (a) 0.01 K; (b) 300 K; (c) 500 K; (d) 700 K.
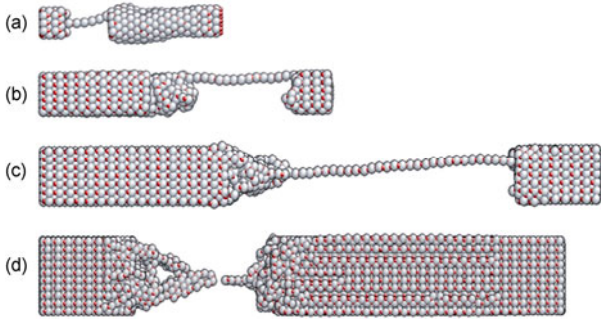
Figure 10 (Color online) Size effect of four typical samples. (a) 10 Å × 10 Å; (b) 15 Å × 15 Å; (c) 20 Å × 20 Å; (d) 30 Å × 30 Å.

2.6 Mechanism

The Arrhenius model could be used to describe the kinetics of an activated process as well as for the process in this paper. The Arrhenius model describes that an energy barrier hinders the forward progress of a reaction (degradation, corrosion, and oxidation). The height of this energy barrier is, effectively, the measure of the resistance to reaction. The explicit description of the Arrhenius equation is as follows:

$$\frac{\dot{\varepsilon}}{\dot{\varepsilon}_0} \ln\left(\frac{\Delta H}{k_B T}\right) = \text{const}, \tag{2}$$

where ΔH is activation enthalpy, k_B is Boltzmann constant, $\dot{\varepsilon}_0$ is characteristic strain rate and could be taken as 1, $\dot{\varepsilon}$ and T is strain rate and absolute temperature, respectively.

From eq. (2), we can conclude that forward progress of the reaction requires the supply of activation energy to surmount this barrier. Thus the rate at which the reaction proceeds depends on the momentum that is provided to surmount the activation energy barrier. During the tensile process of ZnO DC, we found that the temperature and strain rate are two important factors governing the formation of ZnO DC. With the Arrhenius model, we could explain corresponding phenomenon. As shown by the Arrhenius equation, low temperature and high strain rate have the same effect on the process. It has been shown that the high strain rate and low temperature in a limited scope are beneficial to the formation of DC.

2.7 Energy release mechanism

To illuminate the underlying mechanism of the formation of various structures under different combined effects, and to understand why the long DC at low stretching rate is less favored, we note that any single atomic chain structure will have a high energy state due to the very low coordination environment. The creation of such a high energy state could be taken as one method to release the internal strain energy accumulated during the tensile process. However, there are many other methods to release the strain energy through the

formation of other defects, such as through atom dislocations. Thus one assumption is that the way of releasing strain energy by the system depends on how fast its relaxations of certain modes of defects compared to the external loading rate. If the system relaxation of certain type of defect is faster than the external loading rate, the formation of such defect should be dominant in the elongation process [15]. For the simulation in this paper, the strain rate is high, thus the ZnO NWs tend to form DC to release accumulated energy.

3 Vibration modes for ZnO DC

It is well-known that the DC is one simple and classic prototype in condense matter physics [28]. The discovery of MC or DC in various materials makes that prototype from theory to reality for 1-D Lattice diatomic model. Considering a stationary linear DC of atoms in equilibrium (Figure 11), we apply Newton's Second Law and the nearest-neighbor approximation to this system which gives a dispersion relation with two "branches"; acoustic mode (for "+") and optical mode (for "−"),

$$\omega^2 = \beta\left(\frac{M_1 + M_2}{M_1 M_2}\right)$$
$$\pm\left[\beta^2\left(\frac{M_1 + M_2}{M_1 M_2}\right)^2 - \frac{4\beta^2}{M_1 M_2}\sin^2(aq)\right]^{1/2}, \tag{3}$$
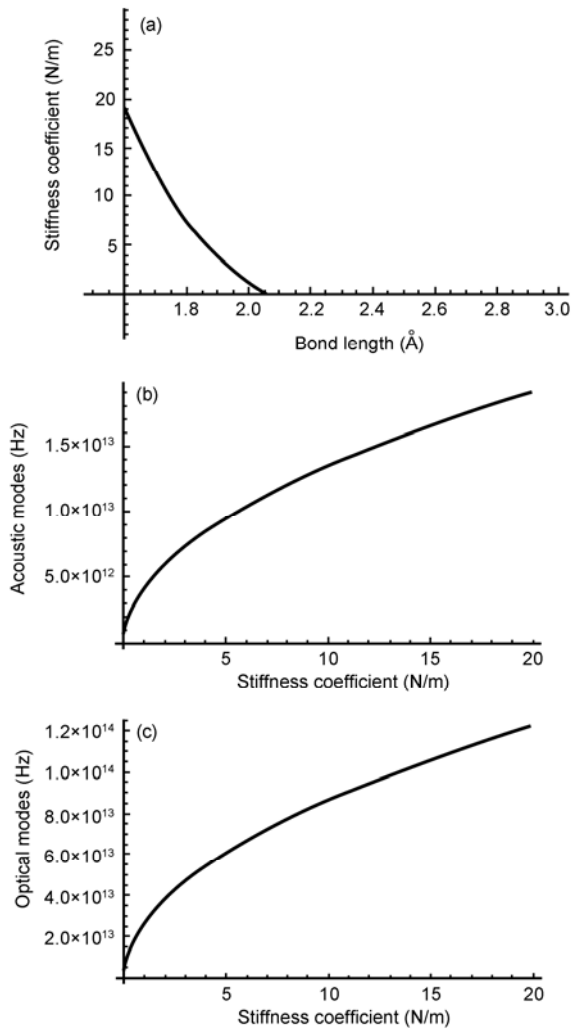
where ω is vibration frequency, β is stiffness coefficient, a is distance between adjacent atoms, M_1 and M_2 are masses of Zn and O atoms.

The relationships among bond length, stiffness coefficient and frequencies of vibration modes are shown in Figure 12. Increasing bond length lead to small interactions between Zn and O atoms, which makes the stiffness coefficient become smaller. With the increase of bond length, the stiffness coefficient decrease gradually and become 0 while bond length is about 2.06 Å, meaning that the limitation length for Zn—O bond is 2.06 Å. Furthermore, the frequencies of both acoustic and optical modes decrease with the increasing bond length. According to simulation results, the bond length of Zn—O bond cannot be maintained during tensile process, but the geometrical structures is constant for steady existing ZnO DC. Considering the vibration patterns of ZnO DC, the ZnO DC may only carry waves with spe-
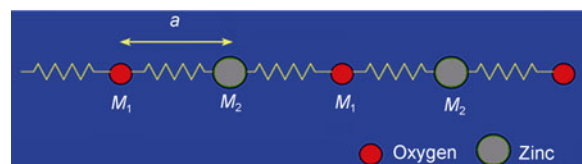
**Figure 11** (Color online) Stationary linear model of ZnO DC.

Figure 12 Relationships among bond length, stiffness coefficient and vibration frequency. (a) Bond length-stiffness coefficient; (b) stiffness coefficient- acoustic mode; (c) stiffness coefficient-optical mode.

cific frequency (acoustic and optical modes), thus the ZnO DC could be applied to fabricate micro wave filter.
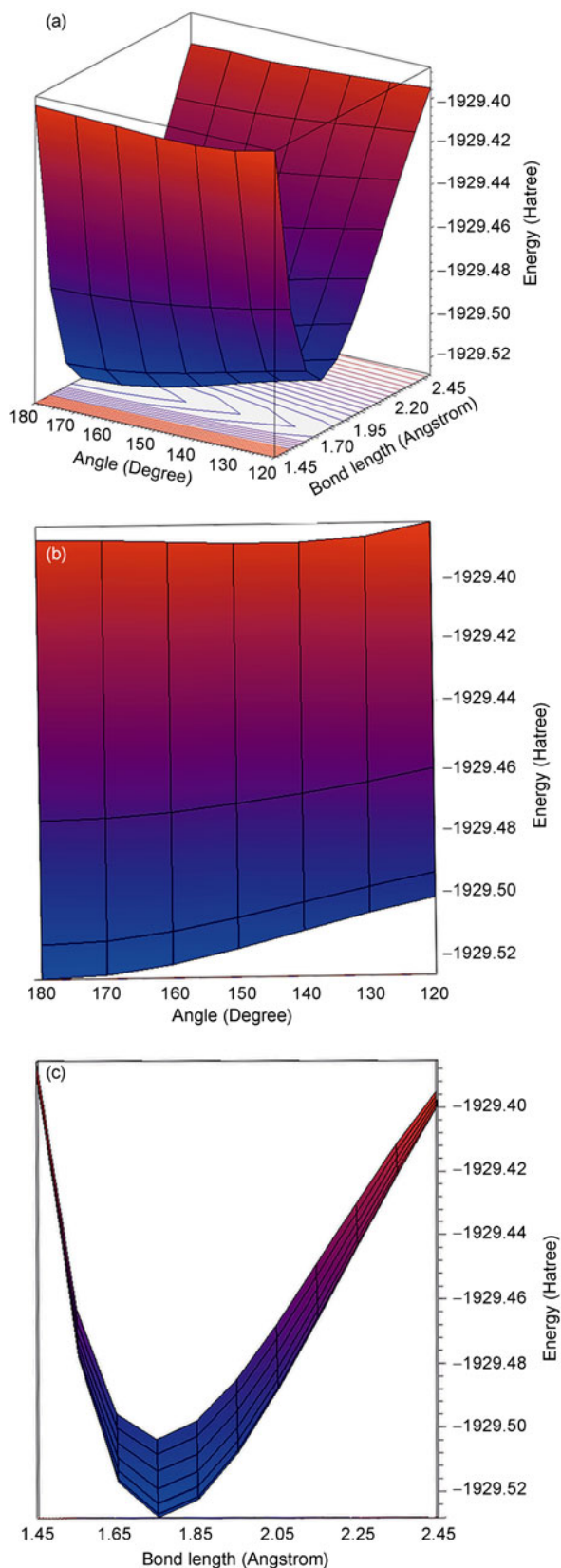
4 Stable structure and *I-V* curve of ZnO DC

The MC has been found in three types: linear, dimers, and zigzag (Figure 13). The fundamental difference between former two types and zigzag is the bond angle. The bond angles between two adjacent bonds is 180° for linear and dimers, while bond angle is less than 180° for zigzag. Bond length is the factor that makes a distinction between linear and dimmers. The adjacent bond length of linear MC is nearly equivalent, while the one bond length is much larger than adjacent bond for dimmers type. To investigate the most stable configuration of one dimensional ZnO diatomic chain, we used DFT calculations implemented in GAUSSION03 [29] to scan its potential surface with respect to the bond length L_{Zn-O} and angle θ_{O-Zn-O}. L_{Zn-O} starts from
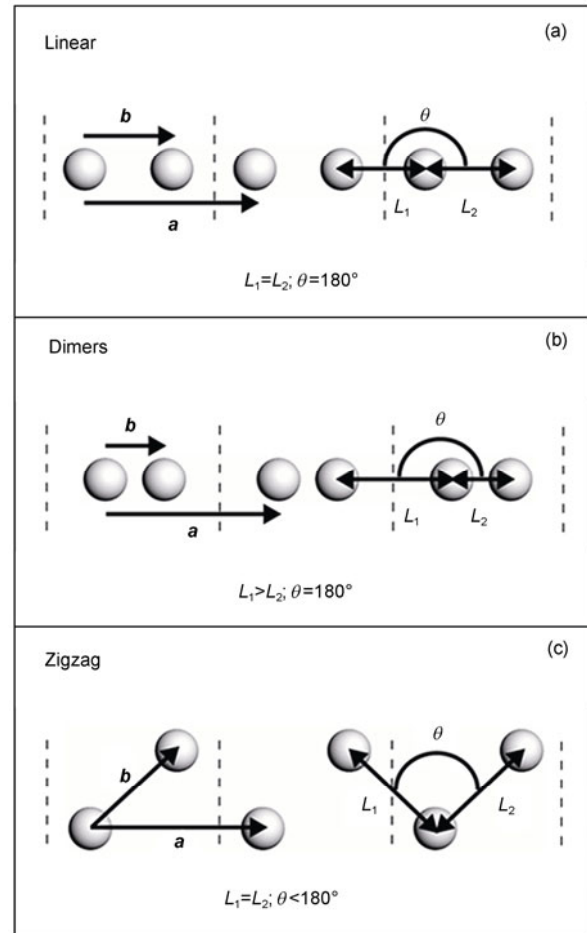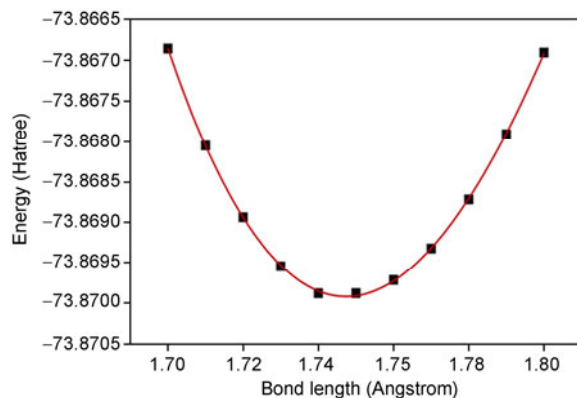

Figure 13   Three types of MC: linear (a), dimers (b), and zigzag (c).

1.45 Å to 2.45 Å with increment of 0.1 Å, θ_{O-Zn-O} starts from 120° to 180° with increment of 10°. B3LYP method with 6-311g basis set was used in order to fully consider the interactions between zinc and oxygen atoms. From the potential surface (Figure 14), we found that the global minimum potential locates at ($L_{Zn-O}\sim1.75$ Å, $\theta_{O-Zn-O}=180°$). The most stable one dimensional ZnO diatomic chain is a linear chain. A more precise scan of the potential surface with respect to L_{Zn-O} when $\theta_{O-Zn-O}=180°$ is performed employing ATK [30] (Figure 15). Making a quadratic fit to these points, the global minimum potential locates at $L_{Zn-O}= 1.745$ Å.

We built a two-probe system (Figure 16(a)) in ATK, whose two probes and scattering region all consist of one dimensional ZnO diatomic chains with $L_{Zn-O}=1.745$ Å. A bias voltage, ranging from 0.0 V to 0.09 V with increment of 0.01 V, was applied between the two probes. Hence, the corresponding current can be calculated according to DFT and non-equilibrium Green's functions (Figure 16(b)). Making a differential of the current to the voltage at $V=0$, zero bias conductance C_0 can be obtained, $C_0=7.68\times10^{-5}$ Siemens. It can be seen by the ATK simulation that the most stable state of ZnO DC is linear as shown in Figure 17.

Figure 15 Potential surface of one-dimensional ZnO DC with respect to the bond length L_{Zn-O} when $\theta_{O-Zn-O}=180°$. Data points are calculated points by ATK, and the solid line is a quadratic fit to these points. The global minimum potential locates at $L_{Zn-O}=1.745$ Å.
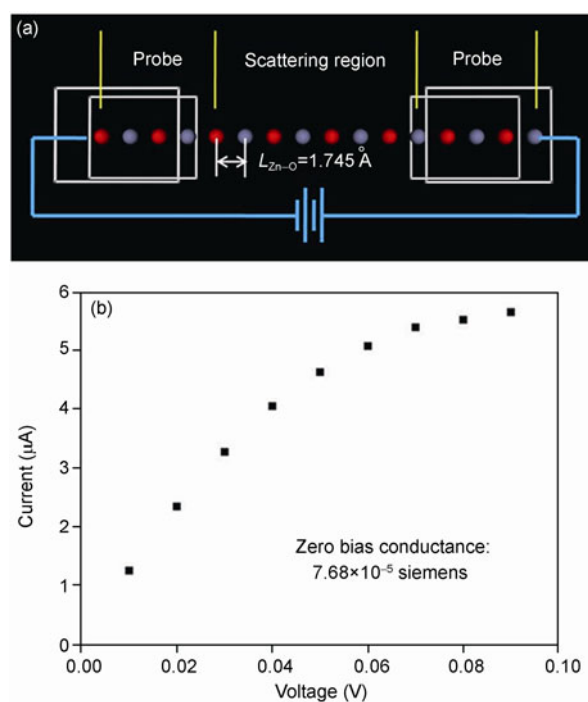
Figure 16 Model of ZnO DC in ATK and simulation result. (a) A two probe system built in ATK. The two probes and the scattering region all consist of one-dimensional ZnO DC; (b) *I-V* curve of one-dimensional ZnO DC.
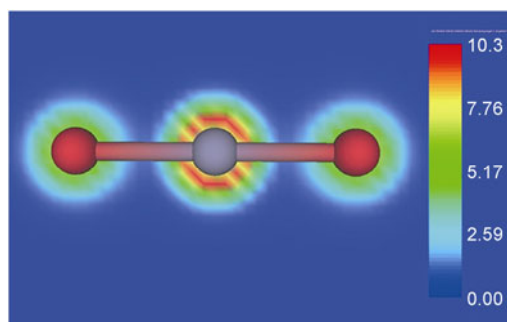
Figure 14 (a) Perspective view of the potential surface of one-dimensional ZnO DC with respect to the bond length L_{Zn-O} and angle θ_{O-Zn-O}; (b) projection of the potential surface on θ-*E* surface; (c) projection of the potential surface on *L-E* surface.

Figure 17 Electron density (ATK). The bond angle between adjacent O—Zn—O bonds is exactly 180°.

5   Conclusions

In this paper, the formation of ZnO DC via MD simulation was studied in detail. The tensile process could be classified into five stages: (a) Homogeneous elongating deformation; (b) Occurrence and propagation of necking; (c) Occurrence of DC; (d) Pulled tight stage; and (e) rupture stage.

Based on our calculation results, it was found that most atoms come from the surface of ZnO NW. Both temperature and strain rate have important effect on the formation of ZnO DC. Too low and too high temperature are not suitable for DC. The effect of strain rate has the similar tendency with temperature, which could be explained by the Arrhenius model and energy release mechanism. Furthermore, size effect was also studied which showed that DC could not form in the small sample and larger sample could produce longer DC. Since the inner atoms have large restriction on the surface atoms, DC is relatively short for even larger samples. However, to increase the activity of surface energy by raising the temperature may be a possible solution for large samples.

Moreover, multi-shell structure formed under tensile strain, and the distance between each layer was about 3 Å which indicates that the attractive force is assumed to be relatively small.

Calculations based on density functional theory in GAUSSION03 showed that the stable configuration for ZnO DC is linear. Furthermore, the *I-V* curve was obtained using ATK.

These architectures, such as ZnO DC and the multi-shell structure of ZnO NW, are intriguing for further exploration of the physical properties and possible applications of advanced molecular or atomic devices using ZnO nanomaterials.

1   Yuan Q Z, Zhao Y P. Topology-dominated dynamic wetting of the precursor chain in a hydrophilic interior corner. Proc Royal Soc A, 2012, 468: 310–322

2   Greer J R. Bridging the gap between computational and experimental length scales: a review on nano-scale plasticity. Rev Adv Mater Sci, 2006, 13: 59–70

3   Ogata S, Umeno Y, Kohyama M. First-principles approaches to intrinsic strength and deformation of materials: perfect crystals, nano-structures, surfaces and interfaces. Modelling Simul Mater Sci Eng, 2009, 17: 013001

4   Ohnishi H, Kondo Y, Takayanagi K. Quantized conductance through individual rows of suspended gold atoms. Nature, 1998, 395: 780–783

5   Sun C Q. Thermo-mechanical behavior of low-dimensional systems: The local bond average approach. Prog Mater Sci, 2009, 54: 179–307

6   Mazzone A M, Rizzoli R. The conductance of monoatomic As and Ag chains deposited onto silicon steps evaluated using a simplified

scattering approach. Physica E, 2007, 37: 292–297

7   Xu B Q, Tao N J. Measurement of single-molecule resistance by repeated formation of molecular junctions**.** Science, 2003, 301: 1221–1223

8   Krawiec M, Jalochowski M. Thermoelectric effects in STM tunneling through a monoatomic chain. Phys Status Solidi B, 2007, 244: 2464–2469

9   Takai Y, Kawasaki T, Kimura Y, et al. Dynamic observation of an atom-sized gold wire by phase electron microscopy. Phys Rev Lett, 2001, 87: 106105

10   Da Silva E Z, da Silva A J R, Fazzio A. How do gold nanowires break? Phys Rev Lett, 2001, 87: 256102

11   Thurmer K, Reutt-Robey J E, Williams E D, et al. Step dynamics in 3D crystal shape relaxation. Phys Rev Lett, 2001, 87: 186102

12   Rodrigues V, Ugarte D. Real-time imaging of atomistic process in one-atom-thick metal junctions. Phys Rev B, 2001, 63: 073405

13   Amorim E P M, da Silva E Z. Helical [110] gold nanowires make longer linear atomic chains. Phys Rev Lett, 2008, 101: 125502

14   Engelund M, Brandbyge M, Jauho A P. Atomistic theory for the damping of vibrational modes in monoatomic gold chains. Phys Rev B, 2009, 80: 045427

15   Sato F, Moreira A S, Coura P Z, et al. Computer simulations of gold nanowire formation: The role of outlayer atoms. Appl Phys A, 2005, 81: 1527–1531

16   Zhu L Y, Wang J L, Ding F. Gold nanotube encapsulation enhanced magnetic properties of transition metal monoatomic chains: An ab initio study. J Chem Phys, 2009, 130: 064706

17   Thiess A, Mokrousov Y, Blugel S, et al. Theory and application of chain formation in break junctions. Nano Lett, 2008, 8: 2144–2149

18   Vélez P, Dassie S A, Leiva E P M. Kinetic model for the long term stability of contaminated monoatomic nanowires. Phys Rev B, 2010, 81: 125440

19   Zarechnaya E Y, Skorodumova N V, Simak S I, et al. Theoretical study of linear monoatomic nanowires, dimer and bulk of Cu, Ag, Au, Ni, Pd and Pt. Comput Mater Sci, 2008, 43: 522–530

20   Velez P, Dassie S A, Leiva E P M. When do nanowires break? A model for the theoretical study of the long-term stability of monoatomic nanowires. Chem Phys Lett, 2008, 460: 261–265

21   Jiang Q, Zhao M, Li J C. Formation of monoatomic chains of metallic elements. Appl Surf Sci, 2003, 206: 331–335

22   Sclauzero G, Dal Corso A, Smogunov A, et al. Interaction of a CO molecule with a Pt monatomic wire: Electronic structure and ballistic conductance. In: Frontiers of Fundamental and Computational Physics: 9th Int Symp, AIP Conf Proc (Sidharth B G., Honsell F, Mansutti O, Sreenivasan K, DeAngelis A, Editors), Vol. 1018. Melville, NY: AIP, 2008. 201–204

23   Kulkarni A J, Zhou M, Ke F J. Orientation and size dependence of the elastic properties of zinc oxide nanobelts. Nanotechnology, 2005, 16: 2749–2756

24   Plimpton S. Fast parallel algorithms for short-range molecular dynamics. J Comput Phys, 1995, 117: 1–19

25   Li J. AtomEye: an efficient atomistic configuration viewer. Modelling Simul Mater Sci Eng, 2003, 11: 173–177

26   Krüger D, Fuchs H, Rousseau R, et al. Pulling monatomic gold wires with single molecules: An *ab initio* simulation. Phys Rev Lett, 2002, 89: 186402

27   Pu Q, Leng Y S, Cummings P T. Rate-dependent energy release mechanism of gold nanowires under elongation. J Am Chem Soc, 2008, 130: 17907–17912

28   Kittel C. Introduction to Solid State Physics. New York: John Wiley & Sons, 1996

29   Frisch M J, Trudes G W, Schlegel H B, et al. Gaussian 09, Revision A.1. Wallingford C T: Gaussian, Inc., 2009

30   Atomistix ToolKit version 2008.11, QuantumWise A/S, 2008. www.quantumwise.com